National Institute of Standards & Technology

Certificate of Analysis

Standard Reference Material® 1979

Powder Diffraction Line Profile Standard for Crystallite Size Analysis
(Nano-Crystalline Zinc Oxide Powder)

This Standard Reference Material (SRM) is intended for use in the analysis of crystallite size through the degree of profile broadening in a powder diffraction experiment. A unit of SRM 1979 consists of two samples of zinc oxide powder, the first with a median crystallite size of approximately 15 nm and a second with a median of approximately 60 nm. These samples are referred to hereafter as the "15 nm crystallites" and "60 nm crystallites" respectively. Each sample contains approximately 3 g of powder bottled in an argon atmosphere.

Material Description: The SRM material was prepared from the decomposition of zinc oxalate through procedures based on those reported by Langford*, et al*. [1]. The specific annealing procedures were tailored to yield the aforementioned two crystallite size ranges. The diffraction profiles of the powders display the effects of stacking faults, as observed by Langford*, et al*., that follow the hexagonal model developed by Warren [2]. The two powders have median particle sizes, measured via laser scattering, of 2.8 μm and 7.7 μm for the 15 nm and 60 nm crystallites respectively; as such, both powders consist of aggregated crystallites. An analysis of diffraction line shape and lattice parameters determined from X-ray powder diffraction data established that the two SRM materials were homogeneous with respect to diffraction properties.

Certified Values: A NIST certified value is a value for which NIST has the highest confidence in its accuracy in that all known or suspected sources of bias have been investigated or taken into account. The measurands are the certified mean column lengths as determined by a Fourier analysis of 22 diffraction lines and the lattice parameters as determined from Pawley analyses. Metrological traceability is to the International System of Units (SI) unit for length (expressed as nanometers). Certified values and uncertainties are provided in Tables 1 through 4, and were calculated according to the method described in the ISO/JCGM Guide [3].

Information Values: The information values for the microstructural parameters obtained from refinements of the data are presented in Table 5. The information data on the particle size distribution, as determined by laser scattering, are given in Figures 1 and 2. An information value is considered to be a value that will be of interest and use to the SRM user, but insufficient information is available to adequately assess the uncertainty associated with the value, or it is a value derived from a limited number of analyses. Information values cannot be used to establish metrological traceability.

Expiration of Certification: The certification of **SRM 1979** is valid indefinitely, within the measurement uncertainty specified, provided the SRM is handled and stored in accordance with instructions given in this certificate (see "Instructions for Storage and Use"). Periodic recertification of this SRM is not required. The certification is nullified if the SRM is damaged, contaminated, or otherwise modified. This material degrades with exposure to humidity. If excessive exposure is suspected, discontinue use.

Maintenance of SRM Certification: NIST will monitor this SRM over the period of its certification. If substantive changes occur that affect the certification, NIST will notify the purchaser. Registration (see attached sheet or register online) will facilitate notification.

Material preparation, measurements, and data analysis leading to the certification of this SRM were provided by J.P. Cline, M.H. Mendenhall, D. Black, and A. Henins of the NIST Materials Measurement Science Division, and J.J. Ritter, formerly of NIST.

R. David Holbrook, Chief
Materials Measurement Science Division

Gaithersburg, MD 20899
Certificate Issue Date: 04 June 2021
Certificate Revision History on Last Page

Steven J. Choquette, Director
Office of Reference Materials

Use of the Advanced Photon Source (APS) at Argonne National Laboratory was supported by the U.S. Department of Energy, Office of Science, Office of Basic Energy Sciences, under Contract No. DE-AC02-06CH11357.

Certain data analysis models were implemented by P.S. Whitfield of Oak Ridge National Laboratory, TN.

TEM analysis was performed by J.E. Bonevich of the NIST Materials Science and Engineering Division.

Statistical analysis was performed by J.J. Filliben of the NIST Statistical Engineering Division.

Support aspects involved in the issuance of this SRM were coordinated through the NIST Office of Reference Materials.

INSTRUCTIONS FOR STORAGE AND USE

Storage: SRM 1979 was bottled in an argon atmosphere. When not in use, store the unused portion of this powder tightly capped in its original bottle, preferably in a dry atmosphere.

Use: The powder of SRM 1979 consists of aggregates of nano-crystallites. If desired, the aggregates can be broken up to a limited extent with a kneading operation using a mortar and pestle without affecting the diffraction line shape.

SOURCE, PREPARATION, AND ANALYSIS[(1)]

The research leading to this SRM, its preparation, characterization, and the certification method are examined in reference 4.

Material Source: The feedstock for SRM 1979 was prepared by decomposing zinc oxalate in a NIST-built vacuum furnace [5]. The precursor zinc oxalate powder, 99.999 % pure (metals basis), was obtained from Alfa Aesar (Ward Hill, MA). The vacuum furnace was designed specifically for this project; it can heat a large quantity of powder, under vacuum, uniformly through the temperature range of 100 °C to 500 °C. The precursor was heated in the vacuum furnace, rapidly from room temperature to 70 °C, then from 70 °C to 110 °C at a rate of 2 °C/h followed by another rapid increase to 250 °C and then up to 400 °C at 2 °C/h. This material was then annealed for a second time in a conventional furnace with no atmospheric control. It was rapidly heated to a temperature of 350 °C, for the 15 nm crystallite size, heated at a rate of 2 °C/h to a final temperature of 400 °C, while the same ramp was used for the 60 nm crystallite size to reach a final temperature of 550 °C.

Certification Method: The certified measurement values of SRM 1979 include the area-weighted mean column lengths, $\langle L \rangle_{area}$, and the volume-weighted mean column lengths, $\langle L \rangle_{vol}$, of the sample contribution to each diffraction profile. Bertaut [6] provides a derivation of the relationship between these parameters and the Fourier transform of the intensity of X-rays reflected from a specimen. Also certified are the lattice parameters. Informational data include the particle size distribution measured via laser scattering and microstructural information determined from the X-ray experiments. The data used for determination of the certified profile breadths were collected on the high-resolution powder diffractometer located on the 11-BM beamline at the APS [7]. The data analyzed to determine the certified lattice parameters, the verification of homogeneity and the information data on microstructure were collected on a NIST-built divergent beam diffractometer (DBD) [8]. This machine was configured with a Johansson incident beam monochromator and either a scintillation or position sensitive detector (PSD). The two machines utilized beam energies of 30 keV and 8.047 keV respectively. SRM 660b *Line Position and Line Shape Standard for Powder Diffraction* [9,10], consisting of lanthanum hexaboride powder, was used to determine the instrument profile function (IPF) for both machines.

Three software packages were used in data analyses: A NIST Python code written for this project that allowed for extraction of Fourier transforms from observed profiles; the commercial code TOPAS [11] was used for the global Pawley [12] analyses, using the fundamental parameters approach (FPA) [13], the Scardi & Leoni model for crystallite size [14] and the Warren model for stacking faults; and lastly the NIST FPA Python Code (FPAPC) [15]. FPAPC duplicated (and independently verified) the capabilities of TOPAS that were used for this study, but also permitted synthesis of Fourier transforms of the diffraction line profiles from the refined parameters (from TOPAS). The linkage of the certified lattice parameter values to the fundamental unit of length, as defined by the SI [16], was established with use of the emission spectrum of Cu Kα radiation as the basis for constructing the diffraction profiles. Certification data were analyzed in the context of both Type A uncertainties, assigned by statistical analysis, and Type B

[(1)] Certain commercial instruments, materials, or processes are identified in this certificate to adequately specify the experimental procedure. Such identification does not imply recommendation or endorsement by the National Institute of Standards and Technology, nor does it imply that the instruments, materials, or processes identified are necessarily the best available for the purpose.

uncertainties, based on knowledge of the nature of errors in the measurements, to result in the establishment of robust uncertainties for the certified values.

Certification Procedure: Ten units of SRM 1979 were removed from the population in accordance to a stratified random protocol. These units consisted of two bottles each; one of the 15 nm material, the second of the 60 nm. For X-ray powder diffraction analyses using the DBD, two specimens were prepared from each bottle of SRM 1979, for a total of 40 specimens. These were run on the DBD using both the scintillation detector and the PSD. Both the order in which the specimens were prepared and the run order were randomized. Data for the measurement of lattice parameters were collected using a zero background quartz plate for the specimen holder. Samples were prepared by kneading a small amount of material in a mortar and pestle using ethanol as a suspending agent. Small amounts of the suspension were transferred to the quartz plate and allowed to dry resulting in a thin film of the zinc oxide powder. With regards to the 11-BM beamline, data were collected from five randomly selected specimens of the 15 nm material while for 60 nm material, data were collected from four specimens. Prior to data collection on the zinc oxide, a dataset from SRM 660b was collected, midway through the data collection, a second dataset from SRM 660b was collected, and a third run was performed when the data collection from the zinc oxide was complete.

With the collection of X-ray powder diffraction data from the DBD, the 1.5 kW copper tube of fine focus geometry was operated at a power of 1.2 kW. The variable divergence incident slit was also set to 0.9°, a 0.2 mm (0.05°) receiving slit was used with the scintillation detector. Data were collected from 25° to 125° 2θ, with a step width of 0.02° 2θ for the 60 nm material, while a width of 0.025 was used with the 15 nm. Likewise, the count times were 16 s and 20 s respectively for a total data collection time of approximately 22 h. The PSD used for this work had a pixel width of 75 μm, and the window width was set to 4 mm. With a goniometer radius of 217 mm these values translate to a resolution 0.02 °2θ and active scan range of 1.05 °2θ. Data were collected in "picture taking" mode wherein data from the PSD window were recorded individually with a combination of coarse steps, in the context of the 1.05 °2θ window, and fine ones, in the context of 0.02 °2θ, resolution. With post data collection processing, this approach allowed for timely data collection at an effective step width of 0.005° 2θ [17]. Scan times were approximately 3.5 h. A 1.5° Soller slit was located in front of the PSD window to limit axial divergence. Samples were spun at 0.5 Hz during data collection. The machine was located within a temperature-controlled laboratory space where the nominal short-range control of temperature was ± 0.1 K. The temperature and humidity were recorded during data collection using Veriteq SP 2000 monitors stated to be accurate to ± 0.15 K. The source was allowed to equilibrate at operating conditions for at least an hour prior to recording any certification data. The performance of the machine was qualified with the use of SRM 660b and SRM 676a *Alumina Powder (Quantitative Analysis Powder Diffraction Standard)* [18] using procedures discussed in reference 8. The 11-BM data were collected from 0.5° to 62° 2θ with a step width of 0.001°; total data collection time was approximately 2 h. Capillary samples were of 0.8 mm in diameter and spun at >90 Hz during data collection.

All data were analyzed using the FPA method as implemented in TOPAS with Pawley analyses. Analysis of data from SRM 660b was performed as part of the calibration of the DBD that also characterized the IPF [8]. Data from the DBD were analyzed using the energies of the Cu $K\alpha_1$ emission spectrum as characterized in reference 19. With the data collected using the scintillation detector, the emission spectrum from the IBM was modeled with a series of Gaussian profiles; three for the $K\alpha_{11}$ line, and a fourth for the $K\alpha_{12}$. With the PSD data, the optics of the Johansson IBM were modeled using dynamical scattering from the monochromator in conjunction with the powder sample as per the optics of a 2-crystal monochromator. The resulting "band pass" model provides a function which effectively cuts off the Lorentzian tails of the native Cu $K\alpha_1$ lines, providing good agreement with the shape of the tails of the observed diffraction profiles. It also adds a dispersion term to the FPA emission model which adds to the width of the modeled lines, further improving the fit to the observation [20]. Parameters associated with the bandpass model, as well as others of the IPF, the incident slit angle and the Soller slit angles of the "full" axial divergence model [21] were refined using scans from SRM 660b. They were then fixed at the SRM 660b values for the analyses of SRM 1979.

The IPF of the 11-BM machine was also modeled with an FPA analysis of SRM 660b. The lattice parameters values were fixed to the certified values. The incident beam spectrum of the 11-BM machine was modeled using three Gaussian profiles with a common, refined wavelength; breadths and intensities were refined independently. The incident beam was considered parallel in the equatorial plane. The "full" axial divergence model [21] was used with the two Soller slit values being refined as a single value. This is not technically correct as the 11-BM machine is not symmetric in the context of the incident vs. diffracted beam path lengths. A quality fit was obtained nonetheless; other, more complex modes of refinement were tested with no improvement. With their refinement, the lengths of the "filament", sample and "receiving slit" were constrained to a common value. Refinements of SRM 660b included a model to account for crystallite size broadening. While this broadening was nearly undetectable for the DBD, it amounted to a substantial portion of the apparent IPF for the 11-BM machine. This crystallite size broadening was not included in subsequent analyses involving the 11-BM IPF, as its true IPF would not include the contributions from the standard. The refined parameters obtained from these analyses of SRM 660b were used as the input data with

FPAPC to compute the Fourier transforms of the IPF at the locations of the ZnO profiles. With this approach, the IPF transforms are noiseless as they are calculated from a theoretical model. However, they do contain the systematic errors that are, in turn, the result of systematic errors of the FPA.

The 11-BM data were analyzed with the a NIST Python code in order to extract the Fourier transforms of the diffraction profiles [22]. This procedure involved a two-step process: the profiles were fit with a Voigt function with the weighting set to favor the fitting of the background, the second involving determining the transform of the residuals. In normal least-squares fitting, one weights the data with $w = 1/\sigma^2 = 1/y$, where y is the number of counts per bin. With this analysis, the data are weighted with $w = 1/(y_0 + y + a^2y^2)$ wherein y_0 is a few counts (to avoid divide-by-zero errors), and a is a parameter that can be varied to increase/decrease the weighting towards the background, typically set to 0.1. With this procedure, an accurate model of the tail region at the expense of the fit in center of each profile was obtained. The residuals are then individually fit with trigonometric functions that map directly into a Fourier series. The Fourier transforms of the observed profiles can then be computed directly. The deconvolution of the IPF from the observed profiles was performed by division, with the NIST Python code, to yield the desired transforms of the sample broadened profiles. Throughout this procedure the statistical errors associated with the original least-squares fits were propagated through to the transforms themselves. Transforms were fit with an analytical function consistent with a log-normal crystallite size distribution to yield the certified MCL values: $\langle L \rangle_{area}$ and $\langle L \rangle_{vol}$.

The FPA analyses of SRM 1979 were carried out with the procedures outlined in reference 8. The crystallite size broadening was modeled with a log-normal size distribution of spherical crystallites using the Scardi and Leoni formalism, and the stacking faults were modeled as per Warren, microstrain was modeled with a Lorentzian profile varying in tan θ. Individual analyses of the DBD data collected with the scintillation detector were performed for homogeneity testing with respect to lattice parameter values. The data from 11-BM, and that collected from the DBD configured with the PSD, were analyzed with global Pawley analyses. There were four such refinements: two for the 15 nm data from each instrument and the analogous two for the 60 nm data. The refined parameters pertinent to the microstructure are shown in Table 5 as information values. Equations developed by Krill and Birringer [23] were used to compute the MCL values shown in Table 5 from the refined parameters of the log-normal distribution. Individual Pawley analyses of the DBD data collected with the PSD were used to generate median and breadth parameters of a log-normal distribution used for homogeneity testing. The certified lattice parameters were obtained from independent analyses of data from specimens mounted as thin films of zinc oxide powder; the sample attenuation function was not included in these analyses. The refined lattice parameters were adjusted using the coefficient of thermal expansion values found in Touloukian *et al.* [24] to values at 22.5 °C.

Certified Values and Uncertainties: The certified values for MCL of the two powders are shown in Tables 1 and 2. FPAPC was used to export the Fourier transforms of the profiles obtained from the refined parameters shown in Table 5. These were then analyzed in an analogous manner as the certified data to yield a second set of MCL values that would correspond to the those obtained with the global FPA Pawley fits using TOPAS. The type B errors were assessed with a graphical comparison of these data to the certified values. The trends observed indicated a 15 % uncertainty was appropriate for the $\langle L \rangle_{area}$ values while the uncertainty for the $\langle L \rangle_{vol}$ MCL values was 10 %. The interval defined by the certified value and its uncertainty represents an expanded uncertainty using $k = 2$, in the absence of systematic error, and was calculated according to the method described in the ISO/JCGM Guide [3]. The measurand is the MCL, area, and volume weighted. The certified values for lattice parameters are provided in Tables 3 and 4. The measurand is the lattice parameters obtained with TOPAS. The components of uncertainty that were evaluated as Type B uncertainties were considered primarily in the context of the uniformity in lattice parameter as a function of 2θ angle; this, in turn, would reflect the functionality of the FPA model. Type A + B uncertainties (statistical + systematic) are shown in Tables 3 and 4.

Table 1. Certified Mean Column Length Values for the 15 nm Zinc Oxide of SRM 1979
(Peak Position Information Values Computed from Certified Lattice Parameters and Cu $K\alpha_1$ = 0.154 059 29 nm)

2θ (°)	hkl	$\langle L \rangle_{area}$ (nm)	Type A (k = 2)	Type A + B (k = 2)	$\langle L \rangle_{vol}$ (nm)	Type A (k = 2)	Type A + B (k = 2)
31.770	010[a]	18.4	± 0.22	± 3.0	26.5	± 0.22	± 2.9
34.409	002[a]	18.9	± 0.22	± 3.1	28.6	± 0.16	± 3.0
36.252	011	14.7	± 0.18	± 2.4	23.5	± 0.22	± 2.6
47.531	012	8.3	± 0.11	± 1.4	16.3	± 0.24	± 1.9
56.598	110[a]	19.2	± 0.65	± 3.5	26.1	± 0.17	± 2.8
62.840	013	11.2	± 0.13	± 1.8	20.1	± 0.17	± 2.2
66.379	020[a]	16.4	± 0.81	± 3.3	24.7	± 0.31	± 2.8
67.942	112[a]	16.1	± 0.21	± 2.6	24.8	± 0.13	± 2.6
69.088	021	15.5	± 1.05	± 3.4	23.4	± 0.44	± 2.8
72.536	004[a]	18.8	± 0.91	± 3.7	26.7	± 0.31	± 3.0
76.955	022	9.4	± 0.12	± 1.5	17.8	± 0.19	± 2.0
81.357	014	7.8	± 0.59	± 1.8	14.5	± 0.35	± 1.8
89.599	023	11.1	± 0.09	± 1.8	19.7	± 0.18	± 2.2
92.798	210[a]	14.1	± 0.11	± 2.2	22.9	± 0.21	± 2.5
95.310	211	13.2	± 0.12	± 2.1	22.0	± 0.11	± 2.3
98.591	114[a]	13.6	± 0.12	± 2.2	23.3	± 0.12	± 2.5
102.931	212	9.4	± 0.14	± 1.6	17.8	± 0.20	± 2.0
104.088	015	10.3	± 0.87	± 2.4	18.7	± 0.30	± 2.2
107.410	024	8.5	± 0.35	± 1.6	15.3	± 0.36	± 1.9
110.394	030[a]	14.3	± 0.22	± 2.4	22.9	± 0.08	± 2.4
116.263	213	10.8	± 0.11	± 1.7	19.4	± 0.15	± 2.1
121.563	032[a]	13.6	± 0.30	± 2.3	22.3	± 0.20	± 2.4

[a] Breadth unaffected by stacking faults.

Table 2. Certified Mean Column Length Values for the 60 nm Zinc Oxide of SRM 1979
(Peak Position Information Values Computed from Certified Lattice Parameters and Cu $K\alpha_1$ = 0.154 059 29 nm)

2θ (°)	hkl	$\langle L \rangle_{area}$ (nm)	Type A (k = 2)	Type A + B (k = 2)	$\langle L \rangle_{vol}$ (nm)	Type A (k = 2)	Type A + B (k = 2)
31.766	010[a]	76.1	± 4.11	± 15.5	112.4	± 1.59	± 12.8
34.419	002[a]	75.5	± 0.95	± 12.3	106.0	± 1.42	± 12.0
36.251	011	67.7	± 0.72	± 10.9	101.7	± 1.40	± 11.6
47.535	012	39.6	± 0.55	± 6.5	76.0	± 1.19	± 8.8
56.591	110[a]	71.6	± 0.56	± 11.3	106.5	± 1.26	± 11.9
62.852	013	52.1	± 4.34	± 12.2	84.0	± 2.03	± 10.4
66.371	020[a]	57.6	± 5.35	± 14.0	97.0	± 3.22	± 12.9
67.942	112[a]	63.7	± 0.62	± 10.2	97.7	± 1.25	± 11.0
69.081	021	61.1	± 0.45	± 9.6	96.6	± 1.06	± 10.7
72.559	004[a]	63.3	± 0.96	± 10.5	95.9	± 1.49	± 11.1
76.953	022	44.5	± 4.19	± 10.9	79.1	± 1.72	± 9.6
81.377	014	34.4	± 3.04	± 8.2	66.7	± 2.00	± 8.7
89.604	023	50.0	± 0.69	± 8.2	82.0	± 0.92	± 9.1
92.784	210[a]	48.5	± 0.44	± 7.7	88.7	± 1.28	± 10.2
95.298	211	49.4	± 4.39	± 11.8	87.4	± 2.24	± 11.0
98.608	114[a]	49.9	± 4.44	± 11.9	85.2	± 1.77	± 10.3
102.923	212	41.9	± 3.78	± 10.1	76.6	± 2.03	± 9.7
104.122	015	45.8	± 0.26	± 7.1	75.8	± 1.12	± 8.7
107.425	024	37.4	± 3.07	± 8.7	67.0	± 1.99	± 8.7
110.375	030[a]	56.3	± 0.60	± 9.0	89.6	± 0.72	± 9.7
116.262	213	44.6	± 3.84	± 10.5	78.5	± 2.05	± 9.9
121.549	032[a]	50.9	± 0.54	± 8.2	86.0	± 1.71	± 10.3

[a] Breadth unaffected by stacking faults.

Table 3. Certified Lattice Parameter Values for SRM 1979
(15 nm material)

	Lattice Parameter (nm)	Type A (k = 2)	Type A + B (k = 2)
a	0.324 966 4	± 0.000 004 6	± 0.000 030
c	0.520 833 0	± 0.000 017 2	± 0.000 030

Table 4. Certified Lattice Parameter Values for SRM 1979
(60 nm material)

	Lattice Parameter (nm)	Type A (k = 2)	Type A + B (k = 2)
a	0.324 982 8	± 0.000 007 5	± 0.000 020
c	0.520 675 0	± 0.000 012 4	± 0.000 020

Information Values and Uncertainties: The refined parameters obtained from the FPA Pawley analyses included those that defined the microstructure of the zinc oxide. These values are considered model dependent and, therefore, more prone to bias than the certified MCL values. These are shown in Table 5. The information values for the particle size distributions, as determined by laser scattering, are given in Figures 1 and 2. TEM analysis confirmed the presence and nature of the stacking faults. Also indicated was that the particles of the 15 nm zinc oxide were aggregates of the 15 nm crystallites displaying a clear texture. It was concluded that this texture was reminiscent of the larger parent crystals of zinc oxalate which upon decomposition formed the poly-crystalline aggregates.

Table 5. Refined Microstructural Parameter Information Values for SRM 1979

	15 nm		60 nm	
Parameter	11-BM	DBD	11-BM	DBD
$\langle L \rangle_{area}$ (nm)	23.83(6)	23.77(30)	95.4(4)	80.7(13)
$\langle L \rangle_{vol}$ (nm)	31.39(9)	31.65(46)	138.9(6)	128.3(25)
median diameter (nm)	24.11(4)	23.35(25)	75.0(1)	51.1(4)
distribution width σ	0.397(1)	0.411(4)	0.508(1)	0.58(4)
deformation α	0.001 21(2)	0.001 59(10)	0.000 28(1)	0.000 35(2)
stacking fault β	0.012 59(5)	0.010 82(23)	0.001 57(1)	0.001 47(3)
strain ε_0 / 10^{-6}	200(2)	182(8)	73(1)	12(2)
χ^2/N (GoF)	1.11	1.06	1.04	1.09

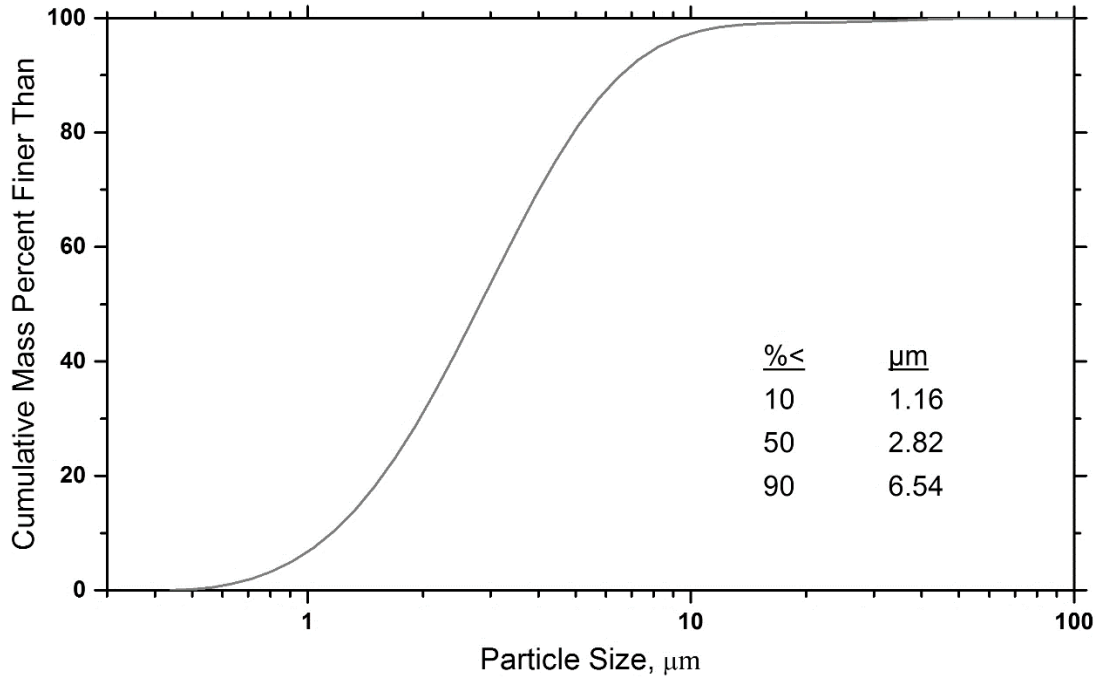

Figure 1. Typical Particle Size Distribution of 15 nm Zinc Oxide by Laser Scattering.

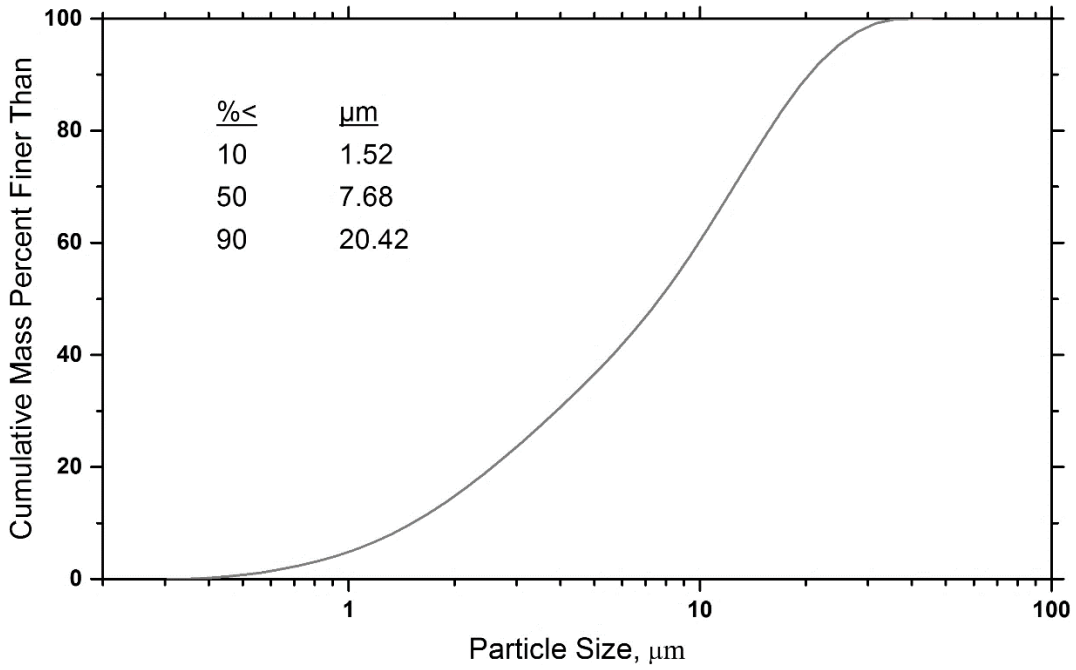

Figure 2. Typical Particle Size Distribution of 60 nm Zinc Oxide by Laser Scattering.

REFERENCES

[1] Langford, J.I.; Boultif, A.; Auffrédic, J.P.; Louër, D.; *The Use of Pattern Decomposition to Study the Combined X-ray Diffraction Effects of Crystallite Size and Stacking Faults in Ex-Oxalate Zinc Oxide*; J. Appl. Cryst., Vol. 26(1), pp. 22–33 (1993).

[2] Warren, B.E.; *X-ray Diffraction*; Addison-Wesley: Reading, MA (1969).

[3] JCGM 100:2008; *Evaluation of Measurement Data — Guide to the Expression of Uncertainty in Measurement* (GUM 1995 with Minor Corrections); Joint Committee for Guides in Metrology (JCGM) (2008); available at https://www.bipm.org/en/publications/guides (accessed Jun 2021); see also Taylor, B.N.; Kuyatt, C.E.; *Guidelines for Evaluating and Expressing the Uncertainty of NIST Measurement Results*; NIST Technical Note 1297; U.S. Government Printing Office: Washington, DC (1994); available at https://www.nist.gov/pml/nist-technical-note-1297 (accessed Jun 2021).

[4] Cline, J.P.; Mendenhall, M.H.; Ritter, J.J.; Black, D.; Henins, A.; Bonevich, J.E.; Whitfield, P.S.; Filliben, J.J.; *The Certification of Standard Reference Material 1979: Powder Diffraction Line Profile Standard for Crystallite Size Analysis*; J. Res. Natl. Inst. Stand. Technol, Vol. 125, No. 125020 (2020).

[5] Cline, J.P.; Leoni, M.; Black, D.; Henins, A.; Bonevich, J.E.; Whitfield, P.S.; Scardi, P.; *Crystalline Domain Size and Faulting in the New NIST SRM 1979 Zinc Oxide*; Pow. Diff. J., Vol. 28(S2), pp. S22–S32 (2013).

[6] Bertaut, E.F.; *Raies de Debye–Scherrer et Repartition des Dimensions des Domaines de Bragg dans les Poudres Polycristallines*; Acta Cryst., Vol. 3(1), pp. 14–18 (1950).

[7] Wang, J.; Toby, B.H.; Lee, P.L.; Ribaud, L.; Antao, S.M.; Kurtz, C.; Ramanathan, M.; Von Dreele, R.B.; Beno, M.A.; *A Dedicated Powder Diffraction Beamline at the Advanced Photon Source: Commissioning and Early Operational Results*; Rev. Sci. Instrum., Vol. 79(8), pp. 085105-1–085105-7 (2008).

[8] Cline, J.P.; Mendenhall, M.H.; Black, D.; Windover, D.; Henins, A.; *The Optics and Alignment of the Divergent Beam Laboratory X-ray Powder Diffractometer and its Calibration using NIST Standard Reference Materials*; J. Res. Natl. Inst. Stand. Technol, Vol. 120, pp. 173–222 (2015).

[9] SRM 660b; *Line Position and Line Shape Standard for Powder Diffraction (Lanthanum Hexaboride Powder)*; National Institute of Standards and Technology; U.S. Department of Commerce: Gaithersburg, MD (25 October 2015).

[10] Black, D.R.; Windover, D.; Henins, A.; Filliben, J.; Cline, J.P.; *Certification of Standard Reference Material 660B*; Pow. Diff. J.; Vol. 26 (2), pp. 155–158 (2011).

[11] Bruker AXS. Topas v5, a component of DIFFRAC.SUITE (2014); available at https://www.bruker.com/en/products-and-solutions/diffractometers-and-scattering-systems/x-ray-diffractometers/diffrac-suite-software/diffrac-topas.html (accessed Jun 2021).

[12] Pawley, G.S.; *EDINP, the Edinburgh Powder Profile Refinement Program*; J. Appl. Cryst., Vol. 13(6), pp. 630–633 (1980).

[13] Cheary, R.W.; Coelho, A.; *A Fundamental Parameters Approach to X-Ray Line-Profile Fitting*; J. Appl. Cryst., Vol 25, pp. 109–121 (1992).
[14] Scardi, P.; Leoni, M.; *Diffraction Line Profiles from Polydisperse Crystalline Systems*; Acta Cryst. A, Vol. 57(5), pp. 604–613 (2001).
[15] Mendenhall, M.H.; Mullen, K.; Cline, J.P.; *An Implementation of the Fundamental Parameters Approach for Analysis of X-ray Powder Diffraction Line Profiles*; J. Res. Natl. Inst. Stand. Technol., Vol. 120, pp. 223–251 (2015).
[16] BIPM; *International System of Units (SI)*; Bureau International des Poids et Mesures; 8th ed.; Sèvres, France (2006); available at https://www.bipm.org/en/publications/guides (accessed Jun 2021).
[17] Mendenhall, M.H.; Cline, J.P.; *Efficient Collection of X-ray Powder Diffraction Data with a Solid State Position Sensitive Detector*; J. Appl. Cryst., submitted.
[18] SRM 676a; *Alumina Powder (Quantitative Analysis Powder Diffraction Standard)*; National Institute of Standards and Technology; U.S. Department of Commerce: Gaithersburg, MD (04 November 2015).
[19] Mendenhall, M.H.; Henins, A.; Hudson, L.T.; Szabo, C.I.; Windover, D.; Cline, J.P.; *High-precision Measurement of the X-ray Cu Kα Spectrum*; J. Phys. B: At. Mol. Opt. Phys., Vol. 50, pp. 115004–115022 (2017).
[20] Mendenhall, M.H.; Black, D.; Cline, J.P.; *The Optics of Focusing Bent-crystal Monochromators on X-ray Powder Diffractometers with Application to Lattice Parameter Determination and Microstructure Analysis*; J. Appl. Cryst., Vol. 52, pp. 1087–1094 (2019).
[21] Cheary, R.W.; Coelho, A.A.; *Axial Divergence in a Conventional X-Ray Powder Diffractometer I. Theoretical Foundations*; J. Appl. Cryst., Vol. 31, pp. 851–861 (1998); see also Cheary, R.W.; Coelho, A.A.; *Axial Divergence in a Conventional X-Ray Powder Diffractometer II, Implementation and Comparison with Experiment*; J. Appl. Cryst., Vol. 31, pp. 862–868 (1998).
[22] Mendenhall, M.H.; Cline, J.P.; *Model-Independent Extraction of the Shapes and Fourier Transforms from Patterns of Partially Overlapped Peaks with Extended Tails*; Acta Cryst., Vol. A75, pp. 158–164 (2019).
[23] Kril, C.E.; Birringer, R.; *Estimating Grain-size Distributions in Nanocrystalline Materials from X-ray Diffraction Profile Analysis*; Philos. Mag. A, Vol. 77(3), pp. 621–640 (1998).
[24] Touloukian, Y.S.; Kirby, R.K.; Taylor, E.R.; Lee, T.Y.R.; *Thermophysical Properties of Matter Volume 13. Thermal Expansion - Nonmetallic Solids*; TPRC Data Series; Plenum Publishing Corp.: New York, NY (1977).

Certificate Revision History: 04 June 2021 (Changes to information values in Table 5; editorial changes); 17 October 2016 (Original certificate date).

Users of this SRM should ensure that the Certificate of Analysis in their possession is current. This can be accomplished by contacting the SRM Program: telephone (301) 975-2200; e-mail srminfo@nist.gov; or via the Internet at https://www.nist.gov/srm.